

Electronic Properties of Transuranium Compounds with HoCoG_{a5}-Type Tetragonal Crystal Structure

Takahiro Maehira¹, Takashi Hotta², Kazuo Ueda³, and Akira Hasegawa⁴

¹Faculty of Science, University of The Ryukyus, Nishihara, Okinawa 903-0213

²Advanced Science Research Center, Japan Atomic Energy Research Institute, Tokai, Ibaraki 319-1195

³Institute for Solid State Physics, University of Tokyo, 5-1-5 Kashiwa-no-ha, Kashiwa, Chiba 277-8581

⁴Niigata University, Niigata 950-2181

(Received March 22, 2024)

By using a relativistic linear augmented-plane-wave method with the one-electron potential in the local-density approximation, we investigate energy band structures and the Fermi surfaces of transuranium compounds NpTG_{a5}, PuTG_{a5}, and AmCoG_{a5} with transition metal atom *ST*. It is found in common that the energy bands in the vicinity of the Fermi level are mainly due to the large hybridization between 5*f* and *G* 4*p* electrons. For PuTG_{a5}, we observe several cylindrical sheets of Fermi surfaces with large volume for *T* = Co, Rh, and Ir. The de Haas-van Alphen (dHvA) frequencies are theoretically estimated for PuCoG_{a5}. It is also found that the Fermi surfaces of NpFeG_{a5}, NpCoG_{a5}, and NpNiG_{a5} are similar to those of UCoG_{a5}, UNiG_{a5}, and PuCoG_{a5}, respectively, except for small details. For AmCoG_{a5}, the Fermi surfaces are found to consist of large cylindrical electron sheets and small closed hole sheets, similar to PuCoG_{a5}. The similarity is basically understood by the change of electron numbers inside the Fermi surfaces on the basis of a rigid-band picture. We discuss our theoretical Fermi surfaces with the dHvA experimental results on NpTG_{a5}.

KEYWORDS: Relativistic linear APW method, Fermi surface, Neptunium compounds, Plutonium compounds, Americium compound

1. Introduction

Recently electronic properties of actinide compounds have attracted renewed attention in the research field of condensed matter physics. Among numerous kinds of actinide compounds, the group of materials with HoCoG_{a5}-type tetragonal crystal structure, frequently referred to as "115", has been intensively investigated both from experimental and theoretical sides. A characteristic trend in the recent investigation of actinide compounds has been a rapid expansion of the research frontier from uranium to transuranium materials, typically found in a series of 115 systems, U-, Np-, Pu-, and Am-115.

First let us briefly survey the properties of U-115. For several transition metal ions *T*, UTG_{a5} are antiferromagnetic (AF) metals or Pauli paramagnets.¹⁽¹²⁾ Among them, neutron scattering experiments have revealed that UNiG_{a5} exhibits the *G*-type AF phase, while UPdG_{a5} and UPTG_{a5} have the *A*-type AF state.^{8,12)} Note that *G*-type indicates a three-dimensional Neel state, while *A*-type denotes a layered AF structure in which spins align ferromagnetically in the *ab* plane and AF along the *c* axis. On the other hand, for *T* = Co, Rh, Ir, Fe, Ru, and Os, magnetic susceptibility is almost independent of temperature, since these are Pauli paramagnets. It is quite interesting that the magnetic structure is different for U-115 compounds which differ only by the substitution of transition metal ions.

Now we move on to transuranium 115 compounds. The rapid progress in the research from uranium to transuranium systems has been triggered by the discovery of superconductivity of Pu-115 compound PuCoG_{a5}.^{13,14)} It has been reported that the superconducting transition

temperature *T_c* of PuCoG_{a5} is 18.5 K, which is an amazingly high value even compared with other well-known intermetallic compounds. The coefficient of electronic specific heat is estimated as $\gamma = 77 \text{ mJ/mol K}^2$, moderately enhanced relative to that for normal metals, suggesting that PuCoG_{a5} should be heavy-fermion superconductor. In PuRhG_{a5}, superconductivity has been also found.¹⁵⁾ Although the value of *T_c* = 8.7 K is lower than that of PuCoG_{a5}, it is still high enough compared with other heavy-fermion superconductors. Another Pu-115 material, PuIrG_{a5}, has been also synthesized, but at least up to now, superconductivity has not been found.¹⁶⁾ In a bulk sample, AF magnetic order has been suggested at low temperatures, while the experimental results have not yet converged due to a problem of sample quality.

Recently Np-115 compounds NpTG_{a5} (*T* = Fe, Co, and Ni) have been synthesized and several kinds of physical quantities have been successfully measured.¹⁷⁽²⁵⁾ Especially, the de Haas-van Alphen (dHvA) effect has been observed in NpNiG_{a5},¹⁸⁾ which is the first observation of dHvA signal in transuranium compounds. For NpCoG_{a5} and NpRhG_{a5}, the dHvA oscillations have been also detected and plural number of cylindrical Fermi surfaces are found.^{20,21)} For NpFeG_{a5}, the magnetic moment at Fe site has been suggested in neutron scattering experiments²⁵⁾ and it has been also detected by ⁵⁷Fe Mössbauer spectroscopy.²⁴⁾ The magnetic structure of Np-115 compounds also depends sensitively on transition metal ion.^{22,25)} *G*-AF for NpNiG_{a5}, *A*-AF for NpCoG_{a5}, and *C*-AF for NpFeG_{a5}. Here *C*-type indicates a situation in which the ferromagnetic chains along the *c* axis are antiferromagnetically coupled in the *ab* plane.

Note also that in the neutron scattering experiment for NpNiGa_5 , the G-AF peak due to canted magnetic moments of Np ions grows after the FM transition occurs.^{22,25)} It is characteristic of U-115 and Np-115 compounds that the magnetic properties are sensitive to the choice of transition metal ions.

Quite recently, the experimental research on actinide 115 systems has been further developed and the frontier has reached americium compound AmCoGa_5 .²⁶⁾ Interestingly enough, from the resistivity measurement, superconductivity has been suggested to occur below 2 K, but unfortunately, it has not been confirmed yet by other experimental techniques, mainly due to the difficulty caused by self-heating effect. It may be interesting to consider a possibility of superconductivity in Am-115 also from the theoretical viewpoint.

In order to elucidate the mechanism of superconductivity and magnetism of such actinide compounds, it is necessary to develop a microscopic theory based on an appropriate f -electron model. A prescription to construct a microscopic f -electron model has been obtained on the basis of a j - j coupling scheme.²⁷⁾ The spirit of the prescription is that the many-body effect is further included into the band-structure calculation results. In actual calculations, since the energy dispersion obtained by the band-structure calculations are very complicated, the f -electron kinetic term is simply reconstructed by using a tight-binding approximation based on the j - j coupling scheme so as to reproduce the band structure around the Fermi energy. Here we note that all 5 f electrons are assumed to be itinerant. Note also that it is quite natural to use the j - j coupling scheme for the construction of the microscopic f -electron model, since the total angular momentum j is the label for one-electron state in the relativistic band-structure calculations in which the Dirac equations are directly solved.

By applying the prescription to uranium compound such as U-115, it has been clarified that electronic structure of uranium compounds is effectively described by a two-orbital Hubbard model based on the j - j coupling scheme.²⁸⁾ With increasing f -electron number, it has been pointed out that this two-orbital Hubbard model can be also applied to some neptunium and plutonium compounds. For instance, quite recently, magnetic structure of Np-115²⁹⁾ and octupole ordering of NpO_2 ³⁰⁾ have been discussed based on the two-orbital Hubbard model.

Although it is important to develop the microscopic analysis of actinide compounds based on the simple f -electron model, close attention should be always paid to correct information about the electronic properties around the Fermi energy obtained by the relativistic band-structure calculations. Those two types of researches, microscopic analysis of the simple f -electron model and band-structure calculations, should be complementary to each other in order to make significant progress in our understandings on magnetism and superconductivity of actinide compounds.

In this paper, we study electronic properties of neptunium, plutonium, and americium compounds such as NpTGA_5 , PuTGA_5 , and AmCoGa_5 by using a relativistic linear augmented-plane-wave (RLAPW) method with

the one-electron potential in the local-density approximation (LDA). We observe that the energy bands in the vicinity of Fermi level are given by the large hybridization between 5 f and Ga 4 p electrons in actinide 115 compounds. For PuTGA_5 , several cylindrical sheets of Fermi surfaces with large volume are found in common for $T = \text{Co, Rh, and Ir}$. For Np-115, we find that the Fermi surfaces of NpFeGa_5 , NpCoGa_5 , and NpNiGa_5 are similar to those of UCoGa_5 , UNiGa_5 , and PuCoGa_5 , respectively. It is also found that the Fermi surfaces of AmCoGa_5 are rather similar to those of PuCoGa_5 . Basically, the similarity is understood by the rigid-band nature of the 115 structure, since the topology of the Fermi surfaces in the band-structure calculations seems to depend on the sum of f -electron number of actinide ions and d -electron number of transition metal ions.

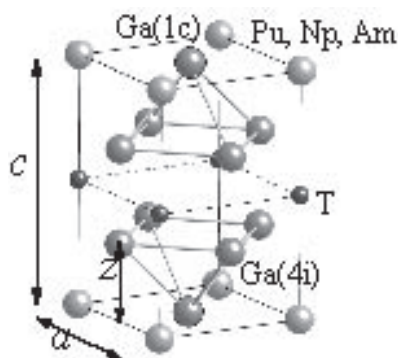
The organization of this paper is as follows. In Sec. 2, we briefly explain the method of our band-structure calculations and lattice parameters for PuTGA_5 , NpTGA_5 , and AmCoGa_5 . In Sec. 3, we show the results for electronic band structure and the Fermi surfaces of PuTGA_5 ($T = \text{Co, Rh, and Ir}$), NpTGA_5 ($T = \text{Fe, Co, and Ni}$), and AmCoGa_5 . In Sec. 4, we will discuss our present results of Pu-, Np-, and Am-115 materials in comparison with that of UCoGa_5 . We also discuss the dHvA results on NpTGA_5 from the band-theoretical viewpoint. Finally, in Sec. 5, we will summarize this paper.

2. Method of Band Calculation

In order to calculate the electronic energy band structure of transuranium compounds, in general, it is necessary to include relativistic effects such as relativistic energy shifts, relativistic screening effects, and spin-orbit interaction.³¹⁾ Based on the Dirac equation, such relativistic effects can be fully taken into account in the energy band structure calculation.³²⁽³⁴⁾ Among several kinds of the band-structure calculation techniques, in this paper we adopt the RLAPW method.³⁵⁾ The exchange and correlation potential is considered within the LDA, while the spatial shape of the one-electron potential is determined in the muffin-tin approximation. The self-consistent calculation is performed by using the lattice constants which are determined experimentally. It is stressed that all 5 f electrons in PuTGA_5 , NpTGA_5 , and AmCoGa_5 are assumed to be itinerant in our band-structure calculations.

In Fig. 1, we show the HoCoGa_5 -type tetragonal crystal structure which belongs to the space group $P4/mmm$ (No. 123) and D_{4h}^{11} . Note that one molecule is contained per primitive cell. In the HoCoGa_5 -type tetragonal structure, positions of atoms in the unit cell are given by (0, 0, 0) for actinide atom, (0, 0, 1/2) for transition metal atom, (1/2, 1/2, 0) for Ga atom at 1c site, and (0, 1/2, z) for Ga atom at 4i site, where z is a parameter determined from X-ray diffraction experiments and the labels for atoms are referred in Fig. 1. The lattice constants, a and c, and the z parameters for NpTGA_5 , PuTGA_5 , and AmCoGa_5 are listed in Tables I and II.

The iteration process for solving the Dirac one-electron equation starts with the crystal charge density that is constructed by superposing the

Fig. 1. Crystal structure of PuTGa_5 , NpTGa_5 and AmCoGa_5 .Table I. Lattice constants and z parameter of NpFeGa_5 , NpCoGa_5 and NpNiGa_5 determined experimentally.^{18,19)}

	NpFeGa_5	NpCoGa_5	NpNiGa_5
a	4.257 Å	4.237 Å	4.231 Å
c	6.761 Å	6.787 Å	6.783 Å
z	0.3011	0.310	0.3135

Table II. Lattice constants and z parameters of PuCoGa_5 , PuRhGa_5 , PuIrGa_5 , and AmCoGa_5 determined experimentally.^{13,15,16,26)}

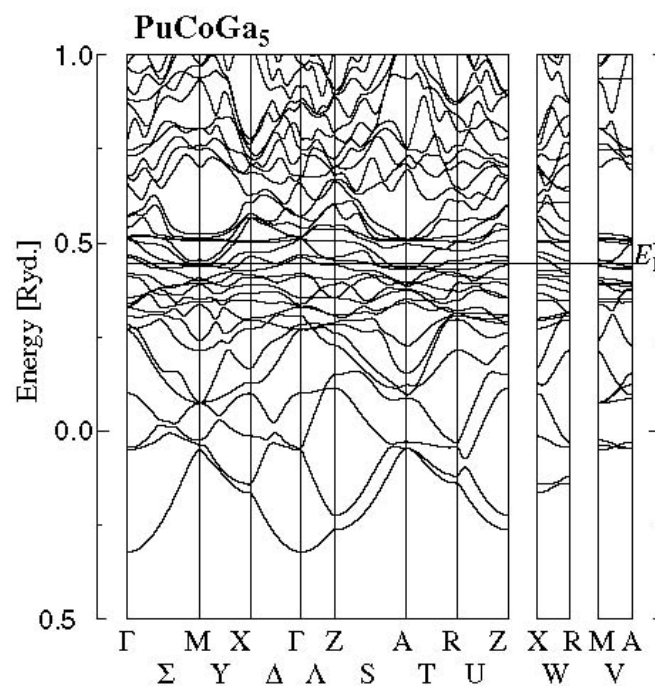
	PuCoGa_5	PuRhGa_5	PuIrGa_5	AmCoGa_5
a	4.232 Å	4.301 Å	4.324 Å	4.233 Å
c	6.786 Å	6.856 Å	6.817 Å	6.823 Å
z	0.312	0.306	0.302	0.3106

Table III. The spin-orbit splitting obtained in the relativistic atomic calculation. Energy unit is milli-Ryd. and 1 Ryd. = 13.6 eV.

Pu 5f	Pu 6d	Np 5f	Np 6d	Am 5f	Am 6d
80	37	70	38	90	36
Fe 3d	Co 3d	Ni 3d	Rh 4d	Ir 5d	Ga 4p
11	13	18	29	90	7

relativistic atomic charge densities for neutral atoms $\text{Pu}(\text{Rn}5f^5 6d^1 7s^2)$, $\text{Np}(\text{Rn}5f^4 6d^1 7s^2)$, $\text{Am}(\text{Rn}5f^6 6d^1 7s^2)$, $\text{Fe}(\text{Ar}3d^6 4s^2)$, $\text{Co}(\text{Ar}3d^7 4s^2)$, $\text{Ni}(\text{Ar}3d^8 4s^2)$, $\text{Rh}(\text{Kr}4d^8 5s^1)$, $\text{Ir}(\text{Xe}4f^{14} 5d^7 6s^2)$, and $\text{Ga}(\text{Ar}3d^{10} 4p^1 4s^2)$, where [Rn], [Kr], [Xe], and [Ar] symbolically indicate the closed electronic configuration for radon, krypton, xenon, and argon, respectively. In the calculation for the atoms, the same exchange and correlation potential are used as for the crystal. We assume that the Rn core state except the $6p^6$ state for Pu, Np, and Am, the Kr core state for Rh, the Xe core state for Ir, the Ar core state for Co, and the Ar core state for Ga are unchanged during the iteration. Namely, the frozen-core approximation is adopted for these core states in the calculation for the crystal. The values of the spin-orbit splitting in the relativistic atomic calculation are listed in Table III.

In each iteration step for the self-consistent calculation

Fig. 2. Energy band structure for PuCoGa_5 calculated by using the self-consistent LAPW method. E_F indicate the position of the Fermi level.

processes, a new crystal charge density is constructed using eighteen k points, which are uniformly distributed in the irreducible $1/16$ part of the Brillouin zone. At each k in the Brillouin zone, 431 plane waves are adopted under the condition $|\mathbf{k} + \mathbf{G}| \leq 4\pi(2/a)$ with \mathbf{G} the reciprocal lattice vector and angular momentum up to $l_{\text{max}} = 8$ are taken into account.

3. Band Calculation Results

3.1 Results for Pu-115

First let us discuss the calculated results for Pu-115 compounds, since PuCoGa_5 and PuRhGa_5 have been recently focused as "high- T_c " f -electron superconductors. Note that a part of the results of PuCoGa_5 has been published.³⁶⁾ Band-structure calculation results for PuTGa_5 ($T = \text{Co, Rh, and Ir}$) were also reported by another group.^{37,38)}

3.1.1 PuCoGa_5

In Fig. 2, we depict the energy band structure along the symmetry axes in the Brillouin zone in the energy region from 0.5 Ryd. to 1.0 Ryd. Note here that the three Pu 6p and twenty-five Ga 3d bands in the energy range between 1.0 Ryd. and 0.6 Ryd. are not shown in Fig. 2, since those bands are irrelevant to the present discussion. The Fermi level E_F is located at 0.446 Ryd. and in the vicinity of E_F , there occurs a hybridization between the Pu 5f and Ga 4p states. Around E_F near M point, the 12 5f bands split into two groups, corresponding to the total angular momentum $j = 5/2$ (lower bands) and $7/2$ (upper bands). The magnitude of the splitting between those groups is estimated as 1.0 eV, which is almost equal to the spin-orbit splitting in the atomic 5f state.

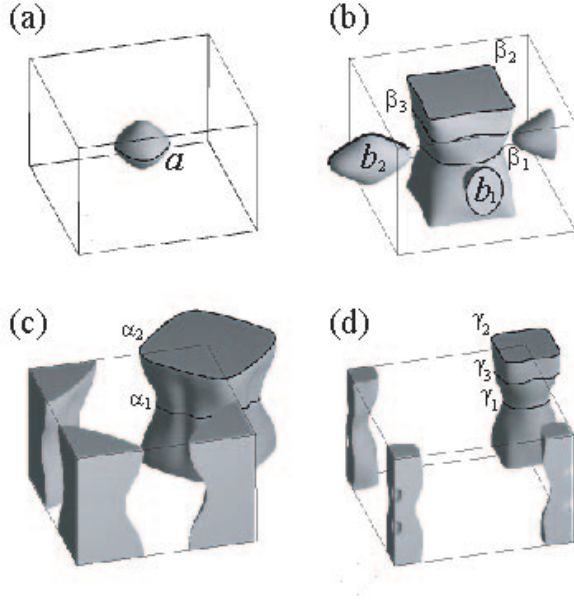


Fig. 3. Calculated Fermi surfaces of PuCoGa₅ for (a) 15th band hole sheets, (b) 16th band hole sheets, (c) 17th band electron sheets, and (d) 18th band electron sheets. The center of the Brillouin zone is set at the Γ point. We also show various kinds of extremal cross section of the Fermi surface.

Table IV. The number of valence electrons for PuCoGa₅ in the Pu APW sphere, the Co APW sphere, and the Ga APW sphere partitioned into angular momenta.

	s	p	d	f
Pu	0.39	6.15	1.81	5.24
Co	0.43	0.44	7.46	0.01
Ga(1c)	0.95	0.69	9.92	0.01
Ga(4i)	3.73	2.82	39.75	0.06

The number of the valence electrons in the APW sphere is partitioned into the angular momenta as listed in Table IV. There are 8.17 valence electrons outside the APW sphere in the primitive cell. The total density of states at E_F is evaluated as $N(E_F) = 97.3$ states/Ryd.cell. By using this value, the theoretical specific heat coefficient γ_{band} is estimated as $16.9 \text{ mJ/K}^2 \text{ mol}$. We note that the experimental electronic specific heat coefficient γ_{exp} is $77 \text{ mJ/K}^2 \text{ mol}$.¹³⁾ We define the enhancement factor for the electronic specific heat coefficient as $\gamma_{\text{band}}/\gamma_{\text{exp}} = 1$, and in the present case, we obtain $\gamma_{\text{band}}/\gamma_{\text{exp}} = 3.6$. The disagreement between γ_{band} and γ_{exp} values is ascribed to electron correlation effect and electron-phonon interactions, which are not fully taken into account in the present LDA band theory.

Now let us discuss the Fermi surfaces of PuCoGa₅. In Fig. 2, the lowest fourteen bands are fully occupied. The next four bands are partially occupied, while higher bands are empty. Namely, 15th, 16th, 17th, and 18th bands crossing the Fermi level construct the hole or electron sheet of the Fermi surface, as shown in Fig. 3. The Fermi surface from the 15th band consists of one hole sheet centered at the Γ point. The 16th band has two

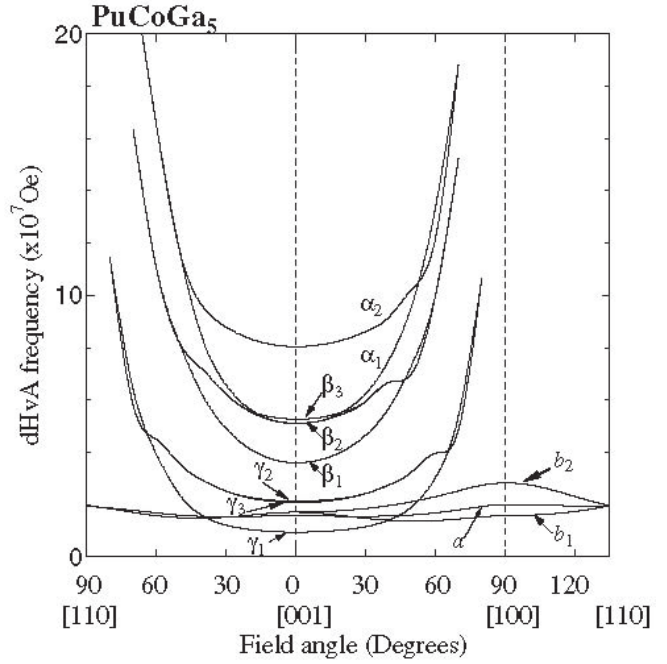


Fig. 4. Angular dependence of the theoretical dHvA frequency in PuCoGa₅. The labels of the branches are referred in Fig. 3.

kinds of sheets, as shown in Fig. 3(b). One is a set of small hole pockets, each of which is centered at the Γ point. Another is a large cylindrical hole sheet which is centered at the Γ point. The 17th band forms a large cylindrical electron sheet which is centered at the M point. The 18th band has a slender cylindrical electron sheet which is also centered at the M point. These electron sheets are characterized by two-dimensional Fermi surfaces. The number of carriers contained in these Fermi surface sheets are 0.040 holes/cell, 0.563 holes/cell, 0.519 electrons/cell, and 0.084 electrons/cell in the 15th, 16th, 17th, and 18th bands, respectively. The total number of holes is equal to that of electrons, which represents that PuCoGa₅ is a compensated metal.

Note that the Fermi surfaces of PuTGA₅ are similar to those of CeTIn₅.³⁹⁾ This similarity can be understood based on the electron-hole conversion relation in the $j-j$ coupling scheme,³⁶⁾ since one f electron is included in the $j = 5/2$ sextet for Ce³⁺ ion, while five f electrons are contained for Pu³⁺ ion.

In Fig. 3, various kinds of extremal orbits are depicted on the Fermi surfaces. Among them, a denotes an orbit running around the small closed hole sheet centered at the Γ point in the 15th band, while b_1 and b_2 indicate a couple of dHvA frequency branches which originate from the 16th hole sheets and exist in the narrow range from 0.015 MOe and 0.03 MOe. Its center is located at the Γ point. On the other hand, γ_1 and γ_2 are the orbits running around the cylinder along the V axis in the 17th band, while β_1 , β_2 , and β_3 are the orbits running around the cylinder along the V axis in the 16th band. Finally, α_1 , α_2 , and α_3 denote the orbits running around the cylinder along the V axis in the 18th band. These orbits exist in the large range of angles in the vicinity of the $[001]$ direction.

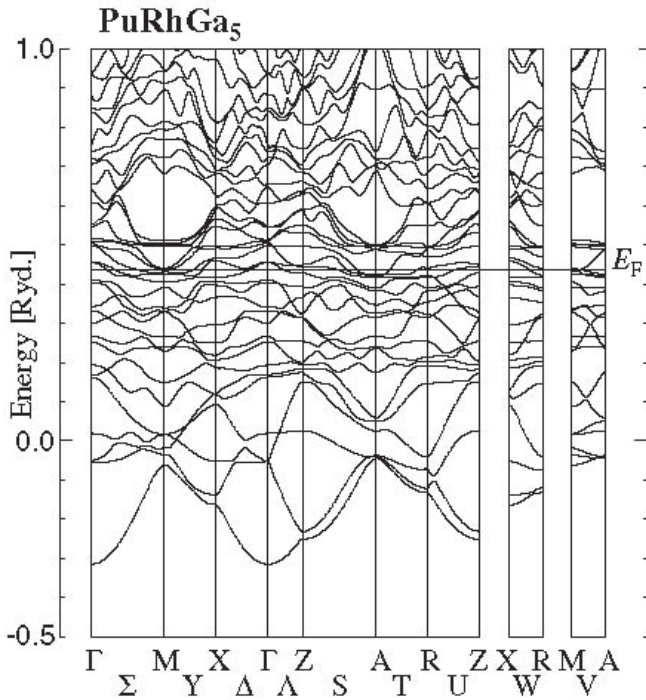


Fig. 5. Energy band structure for PuRhGa_5 calculated by using the self-consistent RLPW method.

Table V. The number of valence electrons for PuRhGa_5 in the Pu APW sphere, the Rh APW sphere, and the Ga APW sphere partitioned into angular momenta.

	s	p	d	f
Pu	0.33	6.16	1.85	5.22
Rh	0.35	0.35	7.38	0.02
Ga (1c)	0.99	0.75	9.94	0.01
Ga (4i)	3.73	2.84	39.77	0.07

In Fig. 4, we show the angular dependence of the theoretical dHvA frequency in PuCoGa_5 . The area of the extremal cross section of the Fermi surface A is related to the dHvA frequency F by the well-known formula $F = (\hbar/2e) A$. The Fermi surface produces many dHvA frequencies in the wide frequency range between 0.01 MOe and 220 MOe, as shown in Fig. 4. The small hole sheet in the 15th band possesses dHvA frequencies in the range between 0.015 MOe and 0.02 MOe. The Fermi surface in the 16th, 17th, and 18th band possesses many extremal cross section in the limited range of angles because of its rugged shape. The dHvA experiments on Pu-115 compounds have not yet been carried out due to several experimental difficulties, but we believe that such experiments will be done in near future. On that occasion, the present theoretical results will be helpful for the experimentalists.

3.1.2 PuRhGa_5

Let us move to another superconducting Pu-115 material PuRhGa_5 . In Fig. 5, we depict the energy band structure and the Fermi energy E_F is located at 0.436 Ryd. Narrow Pu 5f-bands just above E_F are split into two subbands by the spin-orbit interaction. A hybridiza-

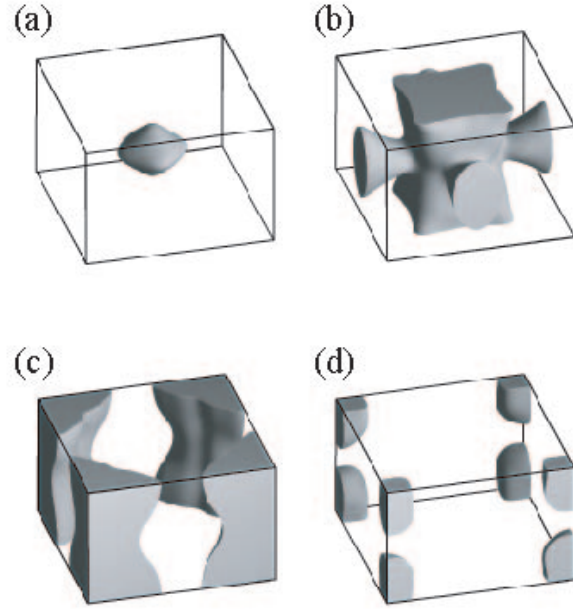


Fig. 6. Calculated Fermi surfaces of PuRhGa_5 for (a) 15th band hole sheets, (b) 16th band hole sheets, (c) 17th band electron sheets, and (d) 18th band electron sheets.

tion between the Pu 5f state and Ga 4p state occurs in the vicinity of E_F also for PuRhGa_5 . In Table V, we list the number of the valence electrons in the APW sphere distributed into the angular momenta. There are 8.31 valence electrons outside the APW sphere in the primitive cell. The theoretical electronic specific-heat coefficient γ_{band} is $13.2 \text{ mJ/K}^2 \text{ mol}$, which is smaller than that of PuCoGa_5 .

Since 15th, 16th, 17th, and 18th bands are partially occupied, these four bands construct the Fermi surface, as in the case of PuCoGa_5 . The hole and electron sheets of the Fermi surface in PuRhGa_5 are shown in Fig. 6. The Fermi surface from the 15th band consists of one hole sheet centered at the Γ point. The hole sheet centered at the Γ point in the 16th band is shown in Fig. 6(b). This Fermi surface possesses the crossed arms, which are connected like a jungle-gym to the next Brillouin zone. The 17th band has a cylindrical electron sheet centered at the M point. The Fermi surface from the 18th band consists of one hole sheet centered at the A point.

The number of carriers contained in these Fermi-surface sheets are 0.040 holes/cell, 0.627 holes/cell, 0.594 electrons/cell, and 0.073 electrons/cell in the 15th, 16th, 17th, and 18th bands, respectively. The total number of holes is equal to that of electrons, since PuRhGa_5 is also a compensated metal.

3.1.3 PuIrGa_5

Now we discuss the electronic properties of yet another Pu-115 compound. In Fig. 7, the energy band structure for PuIrGa_5 in the vicinity of the Fermi energy E_F is shown along high-symmetry axes in the Brillouin zone. The Fermi energy E_F is located at 0.453 Ryd. The band

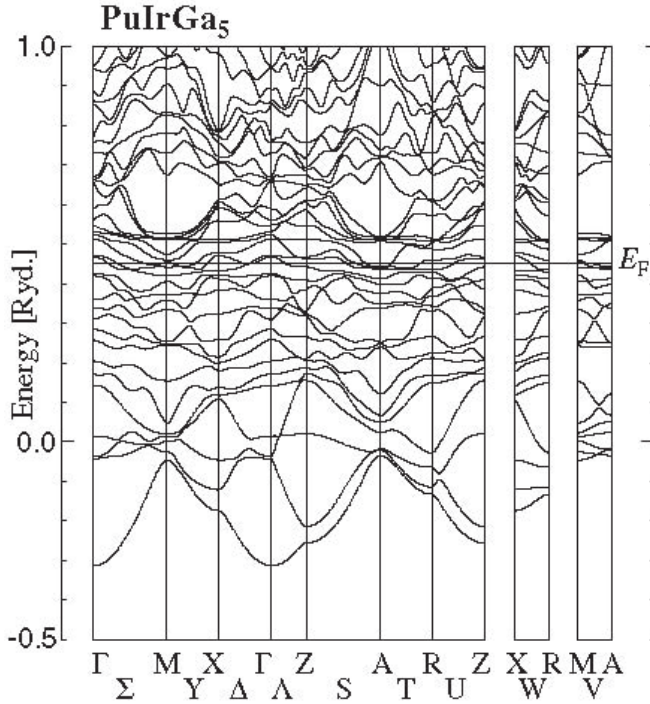


Fig. 7. Energy band structure for PuIrGa₅ calculated by using the self-consistent RLAPW method. E_F indicate the position of the Fermi level.

Table VI. The number of valence electrons for PuIrGa₅ in the Pu APW sphere, the Ir APW sphere, and the Ga APW sphere partitioned into angular momenta.

	s	p	d	f
Pu	0.36	6.13	1.72	5.26
Ir	0.52	0.38	6.93	0.02
Ga(1c)	1.01	0.78	9.96	0.01
Ga(4i)	3.71	2.72	39.76	0.06

structure around the Fermi energy is almost the same as those of PuCoGa₅ and PuRhGa₅. In Table VI, we show the number of the valence electrons in the APW sphere, which are partitioned into the angular momenta. There are 8.64 valence electrons outside the APW sphere in the primitive cell. In each Pu APW sphere, 5.26 electrons with the 5f symmetry are contained. The theoretical electronic specific-heat coefficient_{band} is 11.5 mJ/K² mol, which is smaller than that of PuRhGa₅.

The Fermi level crosses the 15th, 16th, 17th, and 18th bands, which produce various hole and electron sheets of the Fermi surface. The hole and electron sheets of the Fermi surface in PuIrGa₅ are shown in Fig. 8. Again we see that the Fermi surface structure is quite similar to that of PuCoGa₅. The Fermi surface from the 15th band consists of one hole sheet centered at the Γ point. The 16th band has a large cylindrical hole sheet which is centered at the Γ point and two equivalent small hole pockets at the X point. The 17th band has a large electron sheet which is open in the [001] direction and looks like a cylinder running along the V axis. The Fermi surface from the 18th band consists of one hole sheet centered at the A point.

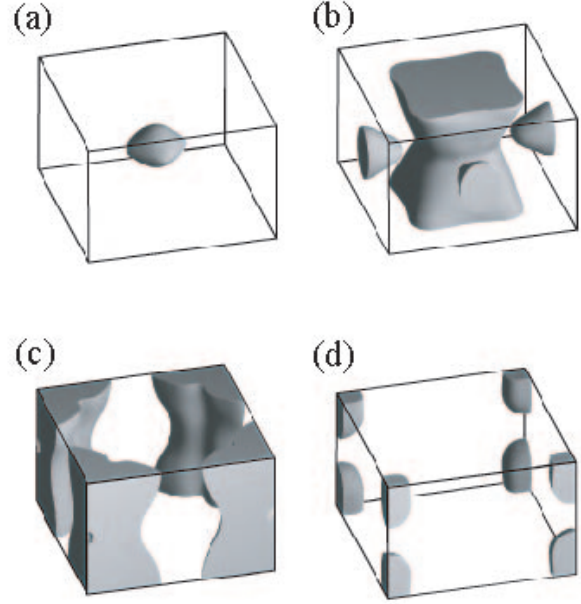


Fig. 8. Calculated Fermi surfaces of PuIrGa₅ for (a) 15th band hole sheets, (b) 16th band hole sheets, (c) 17th band electron sheets, and (d) 18th band electron sheets.

Table VII. The number of valence electrons for NpCoGa₅ in the Np APW sphere, the Co APW sphere, and the Ga APW sphere partitioned into angular momenta.

	s	p	d	f
Np	0.32	6.11	1.91	4.17
Co	0.41	0.43	7.49	0.01
Ga(1c)	0.98	0.73	9.93	0.01
Ga(4i)	3.75	2.90	39.75	0.06

The number of carriers contained in these Fermi-surface sheets are 0.025 holes/cell, 0.579 holes/cell, 0.537 electrons/cell, and 0.067 electrons/cell in the 15th, 16th, 17th, and 18th bands, respectively. The total number of holes is equal to that of electrons, again indicating that PuIrGa₅ is a compensated metal.

Among three Pu-115 compounds, it has been found that there is no essential differences in the Fermi surface structure, when Co is substituted by Rh and Ir. The energy scale of the band-structure calculation is considered to be too large to detect the small change in the Fermi surface structure among three Pu-115 materials.

3.2 Results for Np-115

Let us turn our attention to Np-115 compounds. It is quite impressive that NpTGa₅ with T = Fe, Co, Ni, and Rh have been synthesized and several kinds of physical quantities have been measured. Especially, the dHvA signals have been successfully detected and the comparison with band-calculation results is important. Note that a part of the results on NpCoGa₅ has been reported.^{36,38)}

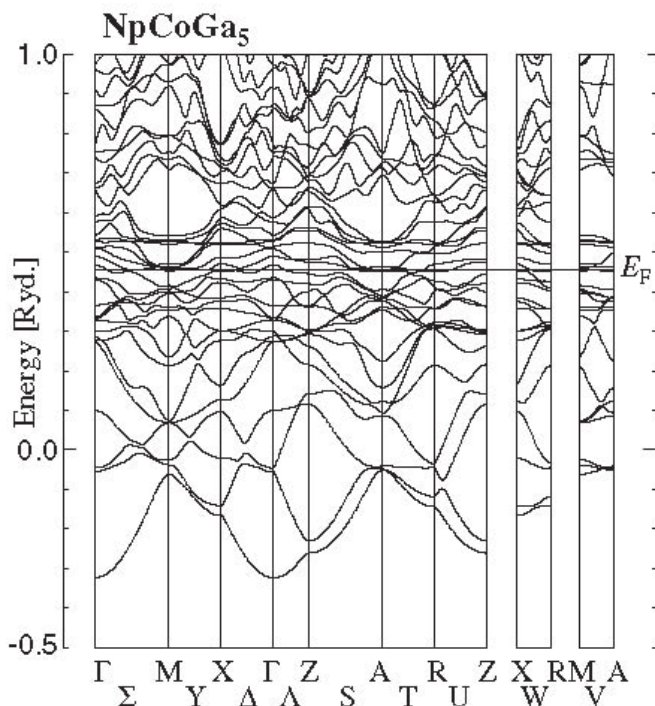


Fig. 9. Energy band structure for NpCoGa₅ calculated by using the self-consistent RLPW method. E_F indicate the position of the Fermi level.

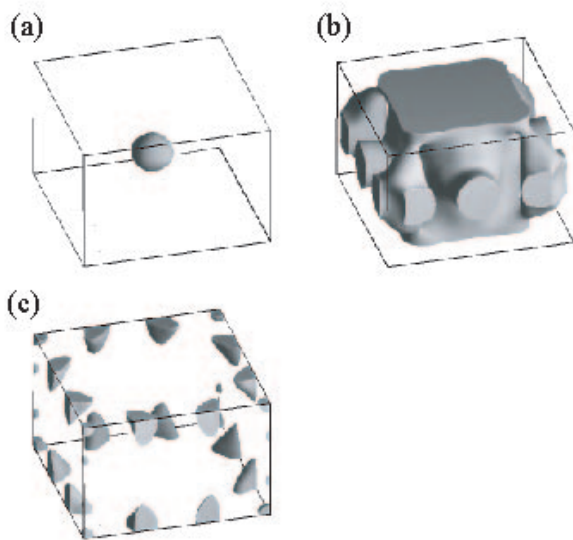


Fig. 10. Calculated Fermi surfaces of NpCoGa₅ for (a) 15th band hole sheets, (b) 16th band hole sheets, and (c) 17th band electron sheets.

3.2.1 NpCoGa₅

First let us show the results of NpCoGa₅. Figure 9 indicates the energy band structure calculated for NpCoGa₅, in the energy range from -0.5 Ryd. to 1.0 Ryd. Note that the three Np 6p and twenty-five Ga 3d bands in the energy range between -1.0 Ryd. and -0.6 Ryd. are not shown in Fig. 9. The Fermi level E_F is located at 0.456 Ryd. and in the vicinity of E_F , there occurs a hybridiza-

tion between the Np 5f and Ga 4p states, similar to the case of PuTGA₅ and UTGA₅. The hybridization between 5f and Ga 4p electrons is considered to be a common feature in actinide 115 materials. In Fig. 9, the flat bands in the narrow energy range just above E_F consist dominantly of the Np f states. Above E_F near M point, the flat 5f bands split into two groups, corresponding to the total angular momentum $j = 5/2$ (lower bands) and $7/2$ (upper bands). The magnitude of the splitting between those groups is estimated as 0.95 eV, a little bit smaller than that of Pu, which is almost equal to the spin-orbit splitting in the atomic 5f state.

The number of the valence electrons in the APW sphere is listed in Table VII. There are 8.11 valence electrons outside the APW sphere in the primitive cell and each Np APW sphere contains about 4.17 electrons in the f state. The total density of states at E_F is evaluated as $N(E_F) = 230.4$ states/Ryd.cell. By using this value, the theoretical specific heat coefficient γ_{band} is estimated as 39.9 mJ/K² mol. Since the experimental electronic specific heat coefficient γ_{exp} is 60.0 mJ/K² mol,⁹⁾ the enhancement factor γ_{enh} is found to be 0.5.

Next we discuss the Fermi surfaces of NpCoGa₅. In Fig. 9, the lowest fourteen bands are fully occupied. The next three bands are partially occupied, while higher bands are empty, indicating that 15th, 16th, and 17th bands crossing the Fermi level form the hole or electron sheet of the Fermi surface, as shown in Fig. 10. The Fermi surface from the 15th band consists of small hole sheets centered at the Γ point. The 16th band constructs a large cylindrical hole sheet centered at the Γ point, which exhibits a complex network consisting of big "arms" along the edges of the Brillouin zone, as observed in Fig. 10(b). The 17th band constructs a small electron sheet, as shown in Fig. 10(c).

The number of carriers contained in these Fermi-surface sheets are 0.015 holes/cell, 0.996 holes/cell, and 0.063 electrons/cell in the 15th, 16th, and 17th bands, respectively. The total number of holes is not equal to that of electrons, indicating that NpCoGa₅ is an uncompensated metal.

3.2.2 NpNiGa₅

Next we discuss the electronic properties of NpNiGa₅. In Fig. 11, the energy-band structure is depicted. We should note that there is no qualitative difference in the energy-band structure between NpCoGa₅ and NpNiGa₅, but the position of E_F is a little bit shifted as $E_F = 0.464$ Ryd. The number of the valence electrons in the APW sphere is listed for each angular momentum in Table VIII. There are 8.44 valence electrons outside the APW sphere in the primitive cell and each Np APW sphere contains about 4.15 electrons in the f state. The total density of states is calculated at E_F as $N(E_F) = 171.9$ states/Ryd.cell, leading to $\gamma_{\text{band}} = 29.8$ mJ/K² mol. Note that $\gamma_{\text{exp}} = 100.0$ mJ/K² mol for NpNiGa₅, leading to $\gamma_{\text{enh}} = 2.4$.

In Fig. 12, we show the Fermi surfaces formed by 15th, 16th, 17th, and 18th bands. The Fermi surface from the 15th band includes one small hole sheet centered at the Γ point. The 16th band constructs a large cylindrical

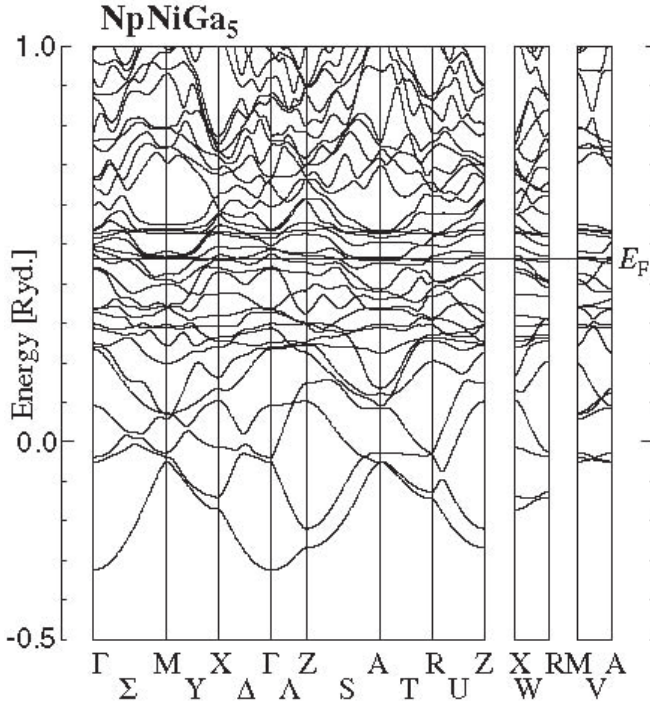


Fig. 11. Energy band structure calculated for NpNiGa_5 with the self-consistent RLPW method.

Table V III. The number of the valence electrons for NpNiGa_5 in the Np APW sphere, the Ni APW sphere, and the Ga APW sphere partitioned into angular momenta.

	s	p	d	f
Np	0.38	6.12	1.91	4.15
Ni	0.48	0.49	8.39	0.01
Ga (1c)	0.94	0.67	9.92	0.01
Ga (4i)	3.72	2.79	39.73	0.05

hole sheet centered at the Γ point, while two equivalent small hole sheets are centered at X points. The 17th band has a large electron sheet centered at the A point. This large electron sheet looks like a swelled square-cushion with bulges on surfaces. The 18th band has a small electron sheet. Each electron sheet lies across the V axis and looks like a cushion. If the 16th-band hole Fermi surface of NpCoGa_5 is almost occupied by an electron and the volume of the 17th-band electron Fermi surface is slightly enlarged, these Fermi surfaces correspond to the 16th-band hole Fermi surfaces and the 17th-band electron ones of NpNiGa_5 , respectively.

The numbers of carriers contained in these Fermi-surface sheets are 0.006 holes/cell, 0.430 holes/cell, 0.427 electrons/cell, and 0.009 electrons/cell in the 15th, 16th, 17th, and 18th bands, respectively. The total number of holes is equal to that of electrons, indicating that NpNiGa_5 is a compensated metal.

3.2.3 NpFeGa_5

Finally, let us discuss the electronic properties of NpFeGa_5 . In Fig. 13, the energy band structure along the symmetry axes in the Brillouin zone is shown. The Fermi energy E_F is located at $E_F = 0.433$ Ryd. Again we

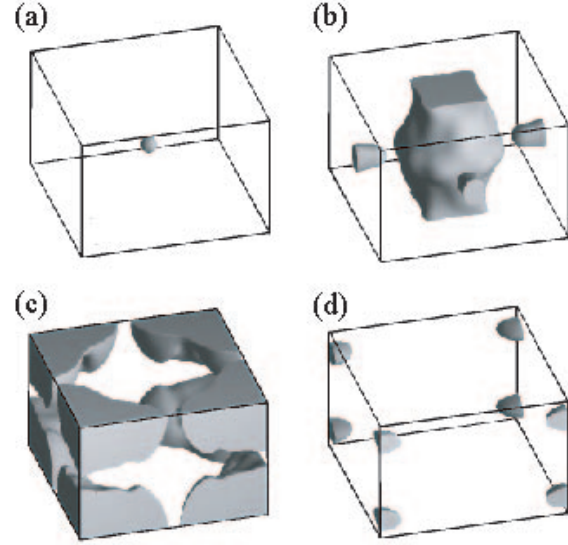


Fig. 12. Calculated Fermi surfaces of NpNiGa_5 for (a) 15th band hole sheets, (b) 16th band hole sheets, (c) 17th band electron sheets and (d) 18th band electron sheets.

Table IX. The number of the valence electrons for NpFeGa_5 in the Np APW sphere, the Fe APW sphere, and the Ga APW sphere partitioned into angular momenta.

	s	p	d	f
Np	0.32	6.04	1.79	4.13
Fe	0.40	0.38	6.40	0.01
Ga (1c)	1.08	0.90	9.98	0.02
Ga (4i)	3.85	2.92	39.79	0.06

observe that the electronic structure of NpFeGa_5 is similar to NpCoGa_5 , except for the location of the Fermi level. The number of the valence electrons in the APW sphere is listed in Table IX. There are 8.03 valence electrons outside the APW sphere in the primitive cell and each Np APW sphere contains about 4.13 electrons in the f state. The total density of states is calculated at E_F as $N(E_F) = 133.6$ states/Ryd.cell, leading to $\chi_{\text{band}} = 23.1$ mJ/K² mol.

We note that the lowest fourteen bands are fully occupied, the next two bands are partially occupied, and higher bands empty. Then, 15th and 16th bands construct the Fermi surfaces, as shown in Fig. 14. These Fermi-surface sheets are small in the size and closed in topology. Note that there exists no open orbit on any sheets. The numbers of carriers contained in these Fermi-surface sheets are 0.094 holes/cell and 0.094 electrons/cell in the 15th and 16th bands, respectively. The total number of holes is equal to that of electrons, which means that NpFeGa_5 is a compensated metal. Note that there are just 0.094 holes/cell and the compensating number of electrons, indicating that NpFeGa_5 is a semimetal.

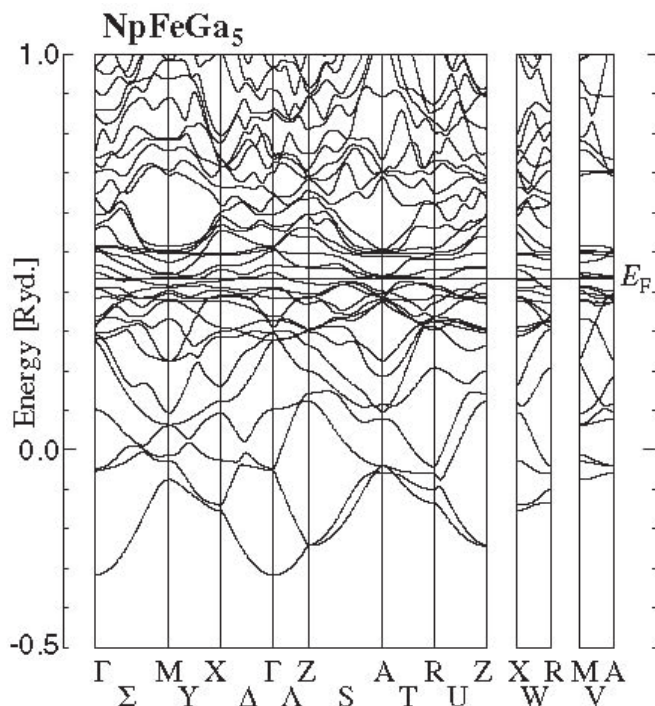


Fig. 13. Energy band structure calculated for NpFeGa_5 with the self-consistent RLAPW method.

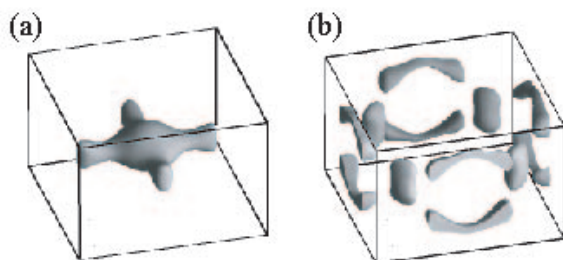


Fig. 14. Calculated Fermi surfaces of NpFeGa_5 for (a) 15th band hole sheets and (b) 16th band electron sheets.

3.2.4 Comment on NpTGa_5

Here we discuss similarity and difference among three Np-115 compounds. For the purpose, let us examine the trend in the change of d electron number in transition metal atoms. The numbers of electrons with the d character contained in the Fe, Co, and Ni APW spheres are 6.40, 7.49, and 8.39 in NpFeGa_5 , NpCoGa_5 , NpNiGa_5 , respectively, indicating clearly that the number is increased by unity among three Np-115 compounds. Since one more d electron is added to NpCoGa_5 , the Fermi level for NpNiGa_5 is shifted upward in comparison with that of NpCoGa_5 .

To understand the change in the electronic properties among three Np-115 compounds, it is useful to see the total density of states (DOS), as shown in Fig. 15. We should note that there is no qualitative difference in the energy-band structure among Np-115 compounds: The 5f bands are split into two subbands by the spin-

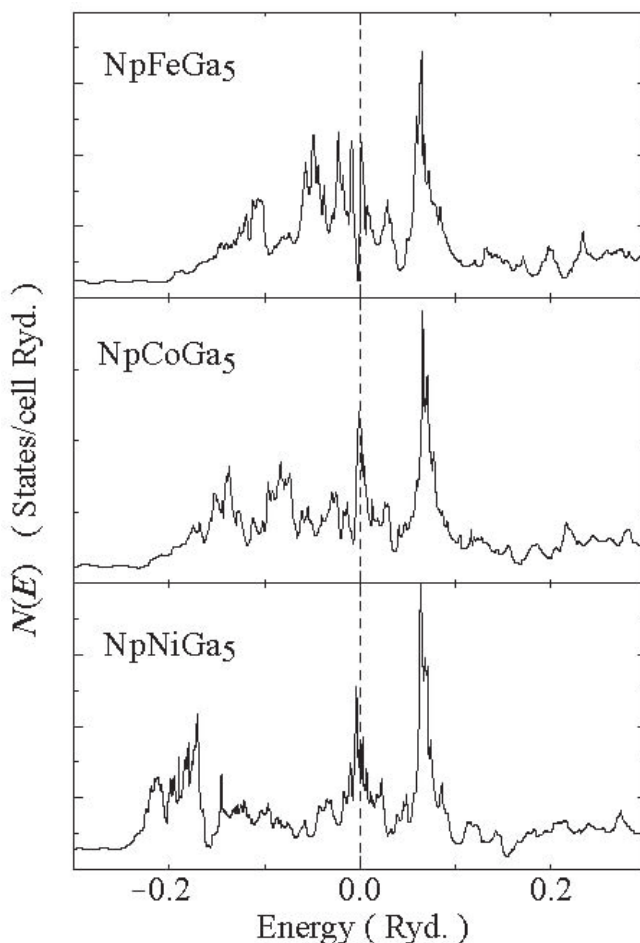


Fig. 15. Density of states for NpFeGa_5 , NpCoGa_5 and NpNiGa_5 . Dashed line indicates the Fermi energy, from which the energy is measured.

orbit interaction and due to the hybridization between 5f and 4p electrons, finite DOS always appear at the Fermi level, indicating that Np-115 compounds are metallic in our band-structure calculations. Note, however, that the peak structure in the DOS are located just at or near the Fermi energy in common with three Np compounds. This fact may be related to the easy appearance of magnetism in Np-115 materials. When the transition metal atom is substituted, the position of E_F is a little bit shifted upward with increasing d electron in the order of NpFeGa_5 , NpCoGa_5 , and NpNiGa_5 .

3.3 Result for AmCoGa_5

Now we show our calculated result of the energy-band structure of AmCoGa_5 within the framework of the itinerant-electron model for the 5f electrons. In Fig. 16, we depict the energy band structure along the symmetry axes in the Brillouin zone in the energy region from 0.5 Ryd. to 1.0 Ryd. We do not show the three Am 6p and twenty-five Ga 3d bands in the energy range between 1.0 Ryd. and 0.6 Ryd. The Fermi level E_F is located at 0.437 Ryd. and in the vicinity of E_F , there occurs a hybridization between the Am 5f and Ga 4p states. The number of the valence electrons in the APW sphere is partitioned into the angular momenta, as listed in Table X. There are 8.22 valence electrons outside the APW

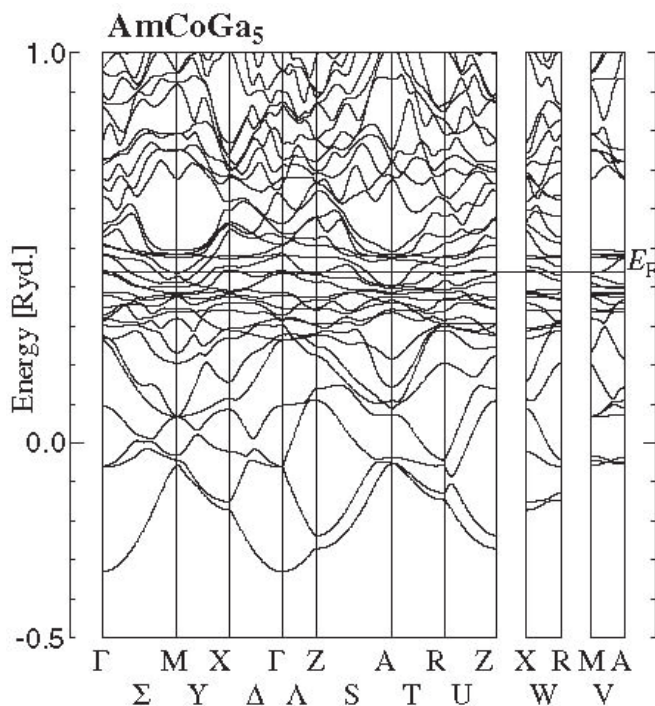


Fig. 16. Energy band structure for AmCoGa₅ calculated by using the self-consistent RLPW method. E_F indicate the position of the Fermi level.

Table X. The number of valence electrons for AmCoGa₅ in the Am APW sphere, the Co APW sphere, and the Ga APW sphere partitioned into angular momenta.

	s	p	d	f
Am	0.39	6.16	1.68	6.39
Co	0.43	0.42	7.45	0.01
Ga (1c)	0.95	0.67	9.92	0.01
Ga (4i)	3.73	2.77	39.75	0.05

sphere in the primitive cell. The total density of states at E_F is evaluated as $N(E_F) = 62.8$ states/Ryd.cell. By using this value, the theoretical specific heat coefficient γ_{band} is estimated as $10.9 \text{ mJ/K}^2 \text{ mol}$.

In Fig. 16, the lowest fifteen bands are fully occupied. The next four bands are partially occupied, while higher bands are empty. Namely, 16th, 17th, 18th, and 19th bands crossing the Fermi level construct the hole or electron sheet of the Fermi surface, as shown in Fig. 17. As shown in Fig. 17(a), the Fermi surface from the 16th band consists of two equivalent small hole sheets centered at the X points and one hole sheet centered at the Γ point. It consists of eight small closed sheets which have the mirror-inversion symmetry with respect of $f100g$, $f010g$, and $f001g$ planes lying between them. The 17th band has three kinds of sheets, as shown in Fig. 17(b). One is a set of two equivalent electron-like pockets, each of which is centered at the R point. Another is electron pocket centered at the Z point. There is also a large cylindrical electron sheet centered at the M point, which characterizes the two-dimensional Fermi surface. The 18th band has a slender cylindrical electron sheet which is also centered at the M point, as shown in Fig. 17(c). The 19th band

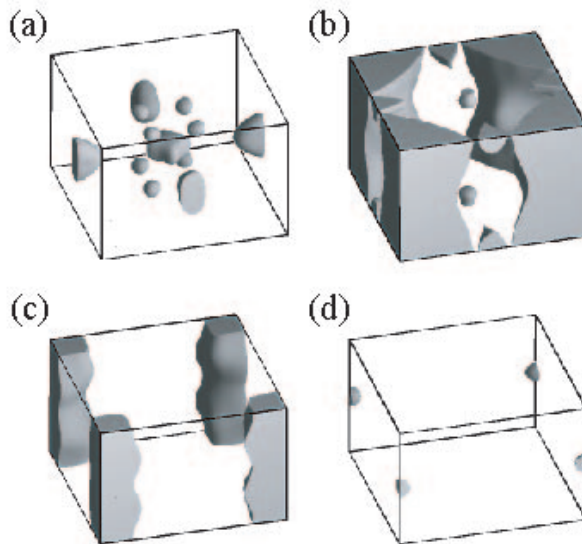


Fig. 17. Calculated Fermi surfaces of AmCoGa₅ for (a) 16th band hole sheets, (b) 17th band hole sheets, (c) 18th band electron sheets, and (d) 19th band electron sheets.

constructs a very small electron sheet, which is centered at the M point, as shown in Fig. 17(d). The number of carriers contained in these Fermi surface sheets are 0.048 holes/cell, 0.785 electrons/cell, 0.272 electrons/cell, and 0.0004 electrons/cell in the 16th, 17th, 18th, and 19th bands, respectively. The total number of holes is not equal to that of electrons, indicating that AmCoGa₅ is an uncompensated metal.

We remark that the Fermi surfaces of AmCoGa₅ seem to be similar to those of PuCoGa₅, since we can see the multiple two-dimensional cylindrical Fermi surface sheets with a constricted part around at M point. For a better understanding of the Fermi surface, we attempt to explain the relationship between AmCoGa₅ and PuCoGa₅. On the basis of the itinerant 5f electron model, AmCoGa₅ has one more Bloch electron per primitive cell in comparison with PuCoGa₅. Therefore, in AmCoGa₅, the Fermi level shifts upward, indicating that relatively the position of 5f bands move downward. As a result, we find that the 15th-band hole sphere of PuCoGa₅ disappears and the size of the 16th-band hole sheet becomes smaller. On the other hand, the sizes of the 17th- and 18th-band cylindrical electron sheets become large. Note that in AmCoGa₅, a small electron sheet appears in the 19th band.

However, in the recent band-structure calculation result, O pahle et al. have found that the Fermi surface structure of AmCoGa₅ is different from that of PuCoGa₅.³⁸⁾ Although the figures for band structure and Fermi surface of AmCoGa₅ were not shown in Ref. 38, their results for PuCoGa₅ have been found to be quite similar to ours and thus, their Fermi surfaces of AmCoGa₅ are considered to be different from ours. One reason for this discrepancy is the treatment of 5f electrons. Namely, we have treated itinerant 5f electrons,

while Ophale et al. considered localized ones. In general, the tendency of localization of 5f electron in Am is stronger than that in Pu, but in actual compounds, it is difficult to determine which is the better approximation, localized or itinerant picture. It will be necessary to clarify which picture well explains the experimental results consistently.

Finally, let us comment on the effect of initial electron configurations in actinide atoms. In the present calculations, as we have mentioned in Sec. 2, we have considered the electron configuration of $([Rn]5f^7 6d^1 7s^2)$ for Am atom. However, this configuration is not uniquely determined. For instance, it may be possible to start the calculation by using $([Rn]5f^7 6d^0 7s^2)$. Also for Np- and Pu-115 compounds, we can consider other electron configurations such as Np $([Rn]5f^6 6d^0 7s^2)$ and Pu $([Rn]5f^6 6d^0 7s^2)$. In order to analyze the Fermi-surface structure of actinide 115 materials, it is necessary to perform carefully further calculations by changing the initial electron configurations for actinide ions. It is an important future task.

4. Discussion

In the previous section, we have shown the band-structure calculation results for PuTGa₅, NpTGa₅, and AmCoGa₅. In order to obtain deep insight into the electronic properties of these 115 compounds, it is useful to compare the results with the electronic energy band structure of UCoGa₅, as shown in Fig. 18.^{40,41)} Note that three U 6p and twenty-five Ga 3d bands are omitted. The Fermi energy E_F is located at $E_F = 0.461$ Ryd. The total density of states at E_F of UCoGa₅ is calculated as $N(E_F) = 48.4$ states/Ryd.cell, which corresponds to $\rho_{\text{band}} = 8.4$ mJ/K² mol.

In UCoGa₅, the 15th and 16th bands form the Fermi surfaces, as shown in Fig. 19. The Fermi surfaces from the 15th band have one sheet centered at the Γ point, two equivalent sheets centered at the X points, and the sheets across the S axis. Figure 19(b) shows a set of the sixteen electron sheets of the Fermi surfaces in the 16th band. Each electron sheet across the T axis looks like a cushion. The total number of holes is equal to that of electrons, which means that UCoGa₅ is a compensated metal.

Except for details, we can observe that the sheets of the Fermi surface of UCoGa₅ with small size and closed topology are similar to those of NpFeGa₅ (see Fig. 14). We also remark that NpCoGa₅ is considered to be UCoGa₅ plus one more f-electron from the viewpoint of the Fermi surface topology, since the small-pocket parts are the remnants of UCoGa₅ and the large-volume Fermi surface contains one additional electron. Interestingly enough, the Fermi surfaces of UNiGa₅⁵⁾ are quite similar to Fig. 10, since both of UNiGa₅ and NpCoGa₅ are regarded as UCoGa₅ plus one more electron, if we simply ignore the difference in the original character, d or f, of the additional one electron. Since NpCoGa₅ is UCoGa₅ plus one f-electron and NpFeGa₅ is regarded as NpCoGa₅ minus one d-electron, the Fermi surfaces of UCoGa₅ are similar to NpFeGa₅.

Based on the discussion on the number of d and f electrons, we also point out that the Fermi surfaces

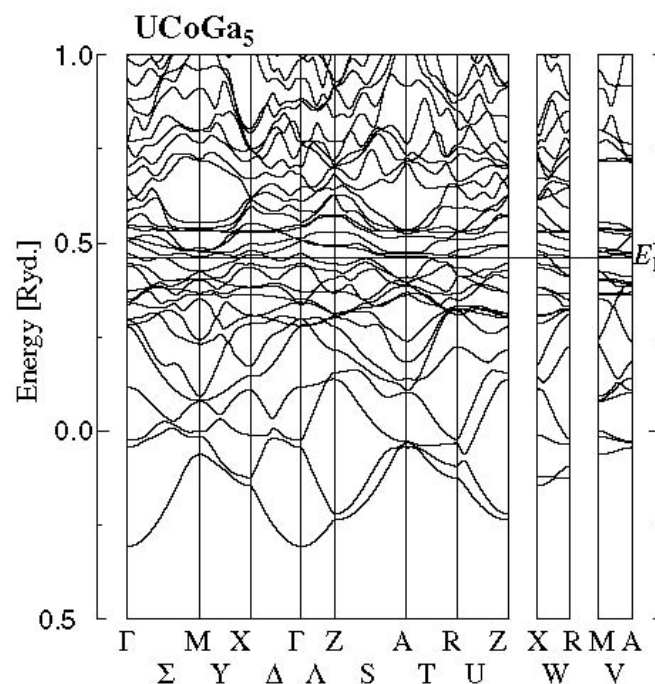


Fig. 18. Energy band structure calculated for UCoGa₅ with the self-consistent RLAPW method.

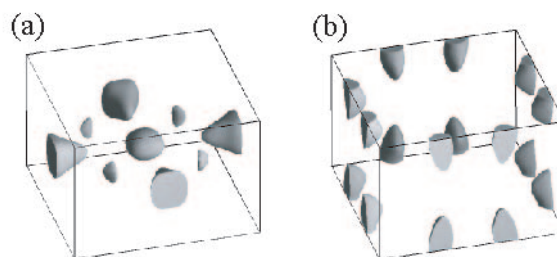


Fig. 19. Calculated Fermi surfaces of UCoGa₅ for (a) 15th band hole sheets and (b) 16th band electron sheets.

of NpNiGa₅ should be similar to those of PuCoGa₅, as shown in Figs. 3 and 12. However, it is clearly observed that two-dimensionality in the Fermi surfaces of NpNiGa₅ becomes worse compared with those of PuCoGa₅. This may be related to the reason why NpNiGa₅ is not superconducting, in spite of the same group with PuCoGa₅ in the electron number discussion.

The above phenomenology on the d- and f-electron numbers seems to suggest that a rigid-band picture works for actinide 115 compounds. This point can be partly validated due to the fact that the band structure of these compounds is basically determined in common by hybridization between broad p bands and narrow f bands in the vicinity of the Fermi level. Based on the rigid-band picture, the electron band structure itself is not changed significantly, even when we change actinide and/or transition metal ions. Thus, just by counting the valence electrons of actinide and transition metal ions, we can easily deduce the Fermi-surface topology, starting with the re-

sults of UCoGa_5 .

It is interesting to compare the total DOS calculated for AnCoGa_5 ($\text{An} = \text{U}, \text{Np}, \text{Pu}, \text{and Am}$), as shown in Fig. 20. We again see that the structures of DOS are qualitatively in common with actinide 115 compounds except for details, when we change the actinide ions. In UCoGa_5 , the Fermi energy is located in a valley, leading to the small DOS at E_F , consistent with a semimetal behavior. On the other hand, for NpCoGa_5 , as mentioned in the previous section, the peak is located just at the Fermi energy. After including the effect of electron correlation, magnetic transition may easily occur in this case. For PuCoGa_5 and AmCoGa_5 , we observe moderate values of the DOS at the Fermi energy, consistent with the paramagnetic metallic phase.

It is noted that the numbers of electrons with the symmetry contained in the actinide APW sphere are, respectively, 3.2, 4.2, 5.2, and 6.4 for UCoGa_5 , NpCoGa_5 , PuCoGa_5 , and AmCoGa_5 , with increasing by unity as the atomic number of actinide atom increases. This fact seems to suggest that electrons are supplied to the unoccupied 5f bands of UCoGa_5 . Namely, the change in the Fermi surface structures among actinide 115 compounds is basically understood by an upward shift of the Fermi level on the rigid electronic bands. The same change occurs between PuCoGa_5 and AmCoGa_5 . Note, however, that it is also important to specify the difference among 115 compounds. Especially, the change of the magnetic structure in Np-115 compounds as well as the appearance of moment at Fe ion in NpFeGa_5 ²²⁽²⁵⁾ is not clarified by the present band-structure calculations. In order to understand these points, it is necessary to calculate not only the total DOS but also the partial DOS for d- and f-electron component within our band-calculation program. It is one of future problems.

Finally, let us discuss the dHvA experimental results on NpNiGa_5 ,¹⁸⁾ NpCoGa_5 ,²⁰⁾ and NpRhGa_5 ,²¹⁾ in comparison with our theoretical Fermi surfaces of Np-115. For NpNiGa_5 , Aoki et al. have observed several sets of the dHvA frequency branches in the region of the order 10^7 Oe, which have the cyclotron effective masses from $1.8m_0$ to $4.9m_0$ in the magnetic field direction $[100]$ and $[001]$. Here m_0 is the rest mass of a free electron. It is remarkable that the effective masses greater than the free-electron mass have been observed, because it implies that the 5f electrons may be itinerant in NpNiGa_5 .

For NpCoGa_5 , a couple of cylindrical sheets of Fermi surfaces with large volume have been detected, while in our band-structure calculations, one cylindrical sheet is obtained, as shown in Fig. 10. Namely, the dHvA results are not explained by the band calculation in the paramagnetic state. A possible explanation for this discrepancy is to consider the folding of Fermi surfaces in the magnetic Brillouin zone, since NpCoGa_5 exhibits the A-type AF structure with a Neel temperature $T_N = 47\text{K}$. If the magnetic unit cell is elongated along the $[001]$ direction and doubled with respect to the chemical unit cell as observed in UPtGa_5 ,¹¹⁾ a quasi-two dimensional Fermi surface is more likely to appear due to the magnetic Brillouin zone.

However, in actual dHvA experiments, due to the ap-

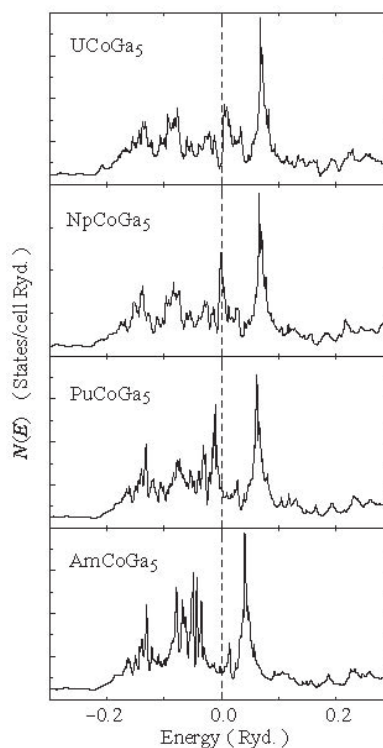


Fig. 20. Density of states for UCoGa_5 , NpCoGa_5 , PuCoGa_5 and AmCoGa_5 . Dashed line indicates the Fermi energy.

plied magnetic field, the system is not AF, but ferromagnetic. Thus, the above explanation cannot be simply applied to this case. In addition, quite recently, the dHvA experiments have been also performed for NpRhGa_5 , which is also A-type antiferromagnet. In this material, four cylindrical sheets of Fermi surfaces have been reported,²¹⁾ consistent with the folding of Fermi surfaces of NpCoGa_5 in the magnetic Brillouin zone. Thus, it is experimentally confirmed that a couple of cylindrical sheets of Fermi surfaces exist in NpCoGa_5 .

It may be true that the rigid-band picture cannot explain universally the band structure of actinide 115 compounds, especially of Np-115 materials. However, a simple tight-binding approximation based on the $j-j$ coupling scheme can reproduce a couple of cylindrical Fermi surfaces,²⁹⁾ by assuming that two of four 5f electrons in Np ion are active. In order to understand the dHvA experimental results on the Fermi surfaces, it is a correct direction to improve the band-structure calculations by considering the difference in the degree of itinerancy among 5f electrons. In fact, it has been suggested that a couple of cylindrical Fermi-surface sheets are obtained in the spin-orbital polarized band-structure calculation.⁴²⁾ Another way is an application of the full-potential method to the fully relativistic band-structure calculations. Such an extension of the band-calculation method is one of important future tasks.

5. Summary

In this paper, we have applied the RLAPW method to the self-consistent calculation of the electronic structure for PuTGa_5 , NpTGa_5 , and AmCoGa_5 on the basis of the itinerant 5f electron picture. It has been found that a

hybridization between the 5f and Ga 4p states occurs in the vicinity of E_F . We have calculated the dHvA frequencies for PuCoGa₅ for future experiments. The similarity in the Fermi surface structure among actinide 115 compounds has been found to be understood based on the rigid-band picture, while the theoretical Fermi surfaces of NpCoGa₅ are different from ones in the recent dHvA experimental results. For the purpose to understand this point, it is a challenging future problem to improve the band-calculation technique.

Acknowledgements

The authors thank F. Wastin for useful information on transuranium 115 compounds. We also thank D. Aoki, Y. Haga, Y. Homma, F. Honda, S. Ikeda, K. Kaneko, K. Kubo, T. D. Matsuda, N. Metoki, A. Nakamura, H. Onishi, Y. Onuki, H. Sakai, Y. Shiokawa, R. E. Walstedt, H. Yamagami, E. Yamamoto, and H. Yasuoka for fruitful discussions. One of the authors (T. H.) has been supported by Grant-in-Aids for Scientific Research (No. 14740219) of Japan Society for the Promotion of Science and for Scientific Research in Priority Areas "Skutterudites" (No. 16037217) of the Ministry of Education, Culture, Sports, Science, and Technology of Japan. The computation of this work has been done using the facilities of Japan Atomic Energy Research Institute.

- 1) Y. N. Grin, P. Rogl and K. Hiebl: *J. Less-Common Metals* 121 (1986) 497.
- 2) V. Sechovsky, L. Havela, G. Schaudy, G. Hilscher, N. Pillmeyer, P. Rogl and P. Fischer: *J. Magn. Magn. Mater.* 104-107 (1992) 11.
- 3) S. Noguchi and K. Okuda: *J. Magn. Magn. Mater.* 104-107 (1992) 57.
- 4) K. Okuda and S. Noguchi: *Physical Properties of Actinide and Rare Earth Compounds*, edited by T. Kasuya, T. Ishii, T. Komatsubara, S. Sakai, N. Mori and T. Saso, *JJAP Series 8* (Publication Office, JJAP, Tokyo, 1993), p. 32.
- 5) Y. Onuki, D. Aoki, P. Wisniewski, H. Shishido, S. Ikeda, Y. Inada, R. Settai, Y. Tokiwa, E. Yamamoto, Y. Haga, T. Maehira, H. Harima, M. Higuchi, A. Hasegawa and H. Yamagami: *Acta Phys. Pol. B* 32 (2001) 3273.
- 6) Y. Tokiwa, Y. Haga, E. Yamamoto, D. Aoki, N. Watanabe, R. Settai, T. Inoue, K. Kondo, H. Harima and Y. Onuki: *J. Phys. Soc. Jpn.* 70 (2001) 1744.
- 7) Y. Tokiwa, T. Maehira, S. Ikeda, Y. Haga, E. Yamamoto, A. Nakamura, Y. Onuki, M. Higuchi and A. Hasegawa: *J. Phys. Soc. Jpn.* 70 (2001) 2982.
- 8) Y. Tokiwa, Y. Haga, N. Metoki, Y. Ishii and Y. Onuki: *J. Phys. Soc. Jpn.* 71 (2002) 725.
- 9) Y. Tokiwa, S. Ikeda, Y. Haga, T. Okubo, T. Izuka, K. Sugiyama, A. Nakamura and Y. Onuki: *J. Phys. Soc. Jpn.* 71 (2002) 845.
- 10) H. Kato, H. Sakai, Y. Tokiwa, S. Kambe, R. E. Walstedt and Y. Onuki: *J. Phys. Chem. Solids* 63 (2002) 1197.
- 11) S. Ikeda, Y. Tokiwa, Y. Haga, E. Yamamoto, T. Okubo, M. Yamada, N. Nakamura, K. Sugiyama, K. Kondo, Y. Inada, H. Yamagami and Y. Onuki: *J. Phys. Soc. Jpn.* 72 (2003) 576.
- 12) K. Kaneko, N. Metoki, N. Bernhoeft, G. H. Lander, Y. Ishii, S. Ikeda, Y. Tokiwa, Y. Haga and Y. Onuki: *Phys. Rev. B* 68 (2003) 214419.
- 13) J. L. Sarrao, L. A. Morales, J. D. Thompson, B. L. Scott, G. R. Stewart, F. Wastin, J. Rebizant, P. Boulet, E. Colineau and G. H. Lander: *Nature (London)* 420 (2002) 297.
- 14) J. L. Sarrao, J. D. Thompson, N. O. Moreno, L. A. Morales, F. Wastin, J. Rebizant, P. Boulet, E. Colineau and G. H. Lander: *J. Phys.: Condens. Matter* 15 (2003) S2275.
- 15) F. Wastin, P. Boulet, J. Rebizant, E. Colineau and G. H. Lander: *J. Phys.: Condens. Matter* 15 (2003) S2279.
- 16) F. Wastin: private communication.
- 17) E. Colineau, P. Javorský, P. Boulet, F. Wastin, J. C. G. Riveau, J. Rebizant, J. P. Sanchez and G. R. Stewart: *Phys. Rev. B* 69 (2004) 184411.
- 18) D. Aoki, E. Yamamoto, Y. Homma, Y. Shiokawa, A. Nakamura, Y. Haga, R. Settai and Y. Onuki: *J. Phys. Soc. Jpn.* 73 (2004) 519.
- 19) D. Aoki, Y. Homma, Y. Shiokawa, E. Yamamoto, A. Nakamura, Y. Haga, R. Settai, T. Takeuchi and Y. Onuki: *J. Phys. Soc. Jpn.* 73 (2004) 1665.
- 20) D. Aoki, Y. Homma, Y. Shiokawa, E. Yamamoto, A. Nakamura, Y. Haga, R. Settai and Y. Onuki: *J. Phys. Soc. Jpn.* 73 (2004) 2608.
- 21) D. Aoki, Y. Homma, Y. Shiokawa, E. Yamamoto, A. Nakamura, Y. Haga, R. Settai and Y. Onuki: preprint.
- 22) F. Honda, N. Metoki, K. Kaneko, D. Aoki, Y. Homma, E. Yamamoto, Y. Shiokawa, Y. Onuki, E. Colineau, N. Bernhoeft and G. H. Lander: to appear in *Physica B*.
- 23) E. Yamamoto, D. Aoki, Y. Homma, Y. Shiokawa, Y. Haga, A. Nakamura and Y. Onuki: to appear in *Physica B*.
- 24) Y. Homma, S. Nasu, D. Aoki, K. Kaneko, N. Metoki, E. Yamamoto, A. Nakamura, S. Morimoto, H. Yasuoka, Y. Onuki and Y. Shiokawa: to appear in *Physica B*.
- 25) N. Metoki: private communication.
- 26) F. Wastin and J. C. G. Riveau: private communication.
- 27) T. Hotta and K. Ueda: *Phys. Rev. B* 67 (2003) 104518.
- 28) T. Hotta: *Phys. Rev. B* 70 (2004) 054405.
- 29) H. Onishi and T. Hotta: to appear in *New J. Phys.*
- 30) K. Kubo and T. Hotta: cond-mat/0409116.
- 31) A. Hasegawa and H. Yamagami: *Prog. Theor. Phys. Suppl.* 108 (1992) 27.
- 32) T. L. Loucks, *Augmented Plane Wave Method* (Benjamin, New York, 1967).
- 33) H. Yamagami and A. Hasegawa: *J. Phys. Soc. Jpn.* 59 (1990) 2426.
- 34) O. K. Andersen: *Phys. Rev. B* 12 (1975) 3060.
- 35) M. Higuchi and A. Hasegawa: *J. Phys. Soc. Jpn.* 64 (1995) 830.
- 36) T. Maehira, T. Hotta, K. Ueda and A. Hasegawa: *Phys. Rev. Lett.* 90 (2003) 207007.
- 37) I. Opahle and P. M. Oppeneer: *Phys. Rev. Lett.* 90 (2003) 157001.
- 38) I. Opahle, S. Elgazzar, K. Koepemik and P. M. Oppeneer: *Phys. Rev. B* 70 (2004) 104504.
- 39) T. Maehira, T. Hotta, K. Ueda and A. Hasegawa: *J. Phys. Soc. Jpn.* 72 (2003) 854.
- 40) T. Maehira, M. Higuchi and A. Hasegawa: *Physica B* 329-333 (2003) 574.
- 41) T. Maehira, M. Higuchi and A. Hasegawa: *J. Phys.: Condens. Matter* 15 (2003) S2237.
- 42) H. Yamagami: to appear in *Physica B*.